Dipion transitions from $X(3872)$ to χ_{cJ} $(J = 0, 1, 2)$

Qi Wu[1], Zhong-Quan Sun[1], Dian-Yong Chen[2,3],* Shi-Dong Liu[4],† and Gang Li[4]‡
[1] *School of Physics, Henan Normal University, Xinxiang 453007, China*
[2] *School of Physics, Southeast University, Nanjing 210094, China*
[3] *Lanzhou Center for Theoretical Physics, Lanzhou University, Lanzhou 730000, China and*
[4] *College of Physics and Engineering, Qufu Normal University, Qufu 273165, China*
(Dated: December 25, 2025)

In this work, we investigate the dipion transition processes $X(3872) \to \pi\pi\chi_{cJ}(J = 0, 1, 2)$ within the framework of heavy hadron chiral perturbation theory, treating $X(3872)$ as a molecular state composed of $D\bar{D}^* + h.c.$ components. By analyzing the box and triangle loop diagrams with nonrelativistic effective field theory power counting rule, we demonstrate that box diagrams dominate these dipion transitions processes. Branching ratios are calculated as functions of the mixing angle θ, which parameterizes the neutral and charged meson compositions of the $X(3872)$. Our results indicate that the branching fractions for $X(3872) \to \pi\pi\chi_{c0}$, $X(3872) \to \pi\pi\chi_{c1}$, and $X(3872) \to \pi\pi\chi_{c2}$ are of orders 10^{-4}, 10^{-3}, and 10^{-5}, respectively. We also predict the ratios $\mathcal{B}[X(3872) \to \pi\pi\chi_{c0/2}]/\mathcal{B}[X(3872) \to \pi\pi\chi_{c1}]$ and $\mathcal{B}[X(3872) \to \pi^+\pi^-\chi_{cJ}]/\mathcal{B}[X(3872) \to \pi^0\pi^0\chi_{cJ}]$. The latter deviates from isospin-symmetry expectations, revealing various degrees of isospin violation. By studying the $\pi^+\pi^-$ and $\pi^+\chi_{cJ}$ invariant mass spectra, we find a double-bump structure in the $\pi^+\pi^-$ invariant mass distributions of the process $X(3872) \to \pi^+\pi^-\chi_{c1}$ and $\pi^+\chi_{c0}$ invariant mass distribution of the process $X(3872) \to \pi^+\pi^-\chi_{c0}$, which could be tested by the future experimental measurements.

Keywords:

I. INTRODUCTION

The exotic hadron state $X(3872)$, discovered by the Belle Collaboration in 2003 in the decay $B^\pm \to K^\pm X(3872)$ with $X(3872) \to \pi^+\pi^- J/\psi$ [1], remains one of the most intriguing puzzles in quantum chromodynamics. It challenges conventional quark model spectroscopy and marks the new era of hadron spectroscopy (see Refs. [2–13] for recent reviews). The J^{PC} quantum numbers of $X(3872)$ have been determined to be 1^{++} [14], which is allowed for the P wave conventional charmonia. However, its mass, measured to be (3871.69 ± 0.17) MeV, is approximately 80 MeV lower than the prediction from Godfrey-Isgur quark model [15], rendering it too light to be the $\chi_{c1}(2P)$ state. Another novel nature of $X(3872)$ is its mass being extremely close to the $D^0\bar{D}^{*0}$ threshold. This proximity strongly suggests that this state possesses a significant $D^0\bar{D}^{*0}$ molecular component [16–21], providing a natural explanation for its exotic properties.

Within the molecular scheme, both the decay and production behaviors of the $X(3872)$ can be naturally accounted for [22–40]. The strongest evidence supporting the molecular hypothesis is the nearly equal branching fractions of the $X(3872) \to \pi^+\pi^- J/\psi$ and $X(3872) \to \pi^+\pi^-\pi^0 J/\psi$ [41–43],

$$\frac{\mathcal{B}[X \to \pi^+\pi^-\pi^0 J/\psi]}{\mathcal{B}[X \to \pi^+\pi^- J/\psi]} = \begin{cases} 1.0 \pm 0.4 \pm 0.3 & \text{Belle} \\ 1.43^{+0.28}_{-0.23} & \text{BESIII} \\ 0.8 \pm 0.3 & \text{BABAR} \end{cases} \quad (1)$$

Measurements of the multi-pion invariant mass distributions reveal the dominate decay pathways: the $\pi^+\pi^- J/\psi$ final state proceeds predominantly via $\rho^0 J/\psi$ [1], while the $\pi^+\pi^-\pi^0 J/\psi$ final state occurs primarily through $J/\psi\omega$. This suggests that the $X(3872)$ couples to both isospin $I = 0$ and $I = 1$ channels with comparable strength, resulting in large isospin violation in these decay patterns. It is reasonable since the charged threshold $D^+D^{*-} + c.c.$ is about 8 MeV above the neutral threshold, and the mass of $X(3872)$ lies so close to the neutral threshold. Numerous studies suggest that the weight of the $D^0\bar{D}^{*0}$ component in $X(3872)$ is over 80% [37, 38, 40, 45–47], despite the important role of the charged $D\bar{D}^*$ components in describing the ratio of the branching fractions of $\rho J/\psi$ and $\omega J/\psi$ channels [48–52].

In addition to the $X(3872) \to \rho^0 J/\psi$, the decays $X(3872) \to \pi^0\chi_{cJ}$ with $J = 0, 1, 2$ are isospin-violated and presumed highly suppressed. It is predicted that the decay rates of pionic transitions from $X(3872)$ to χ_{cJ} are sensitive to the inner structure of the $X(3872)$ [27, 28, 31]. For example, the authors of Ref. [27] first proposed the pionic transitions between $X(3872)$ and χ_{cJ}, and investigated their relative rates under different interpretations of $X(3872)$, particularly, the pure charmonium and four-quark/molecular configurations. Their analysis concluded that: (i) the decay rates are highly suppressed (especially for single-pion transitions); (ii) $X(3872) \to \pi\pi\chi_{c1}$ dominates for charmonium scheme; (iii) single-pion transitions are significantly enhanced in four-quark/molecular scenarios. The authors in Ref. [28] investigated the decays of the $X(3872)$ to P-wave charmonia under the molecular picture and revisited the decay rate of $X(3872) \to \pi\pi\chi_{c1}$ in Ref. [31] by considering a low-energy effective theory for the $X(3872)$ (XEFT). The former work

*Electronic address: chendy@seu.edu.cn
†Electronic address: liusd@qfnu.edu.cn
‡Electronic address: gli@qfnu.edu.cn

[1] Actually, the BESIII Collaboration has measured the ρ^0 and ω contributions to the $X(3872) \to \pi^+\pi^- J/\psi$ decays, and the ρ^0 contribution accounts for 78.6% of the total rate [44].

predicted that dipionic transitions are suppressed by six orders of magnitude relative to single-pion transitions for $J = 0, 2$, with $\mathcal{B}[X(3872) \to \pi^+\pi^-\chi_{cJ}]/\mathcal{B}[X(3872) \to \pi^0\pi^0\chi_{cJ}] \simeq 2$. The latter work revisited the ratio to be $\mathcal{B}[X(3872) \to \pi^0\pi^0\chi_{c1}]/\mathcal{B}[X(3872) \to \pi^0\chi_{c1}] = 10^{-3}$. Considering the $X(3872)$ as a superposition dominated by the molecular $D^0 D^{*0}$ component with additional contributions from $D^{\pm}D^{*\mp}$, $\omega J/\psi$, and $\rho J/\psi$ states, the authors in Ref. [53] calculated the decays $X(3872) \to \pi\chi_{cJ}$ and $X(3872) \to \pi\pi\chi_{cJ}$ as well as the pionic transitions from $X(3872)$ to J/ψ by using the estimated couplings $g_{X\psi\omega}$ and $g_{X\psi\rho}$. The full structure-dependent decay pattern of the $X(3872)$ established in Ref. [53] may help determine its hadronic composition in current and future experiments.

In 2019, the BESIII Collaboration reported the first observation of $X(3872) \to \pi^0\chi_{c1}$, and the central value of the ratio $\mathcal{B}[X(3872) \to \pi^0\chi_{c1}]/\mathcal{B}[X(3872) \to \pi^+\pi^- J/\psi]$ was measured to be 0.88 [54]. Using the PDG value $\mathcal{B}[X(3872) \to \pi^+\pi^- J/\psi] = 4.3\%$ [55], it implies $\mathcal{B}[X(3872) \to \pi^0\chi_{c1}] = 3.8\%$. This branching ratio is comparable to those for $X(3872) \to \pi\pi(\pi)J/\psi$. However, other pionic transitions from $X(3872)$ to P-wave charmonium are kept unknown and only some upper values have been measured. In 2022, the BESIII Collaboration searched for $X(3872) \to \pi^0\chi_{c0}$ and $X(3872) \to \pi^0\pi^0\chi_{c0}$ via $e^+e^- \to \gamma X(3872)$ [56]. The upper limit of these ratios were measured to be

$$\frac{\mathcal{B}[X \to [\pi]\chi_{c0}]}{\mathcal{B}[X \to \pi^+\pi^- J/\psi]} < \begin{cases} 3.6 & [\pi] = \pi^0 \\ 0.56 & [\pi] = \pi^+\pi^- \\ 1.7 & [\pi] = \pi^0\pi^0 \end{cases} \tag{2}$$

at 90% confidence level. Recently, the BESIII Collaboration made further progress in the study of $X(3872) \to \pi\pi\chi_{c1,2}$, and the upper limit of the ratios were measured to be [57, 58],

$$\frac{\mathcal{B}[X \to [\pi\pi]\chi_{cJ}]}{\mathcal{B}[X \to \pi^+\pi^- J/\psi]} < \begin{cases} 0.18 & [\pi\pi] = \pi^+\pi^-, J = 1 \\ 1.1 & [\pi\pi] = \pi^0\pi^0, J = 1 \\ 0.5 & [\pi\pi] = \pi^0\pi^0, J = 2 \end{cases} \tag{3}$$

at 90% confidence level.

The BESIII measurement inspired theoretical studies on the dipionic transitions from $X(3872)$ to χ_{cJ}. In Ref. [59], the decays $X(3872) \to \pi^0\pi^0\chi_{c1}$ and $X(3872) \to \pi^+\pi^-\chi_{c1}$ were estimated in the triangle loop model by considering the $X(3872)$ meson as a $\chi_{c1}(2P)$ charmonium state. The obtained branching fractions of the $X(3872) \to \pi^+\pi^-\chi_{c1}$ and $X(3872) \to \pi^0\pi^0\chi_{c1}$ decays are in order $10^{-5} \sim 10^{-4}$ and their ratio is estimated to be 1.1. However, the contribution from the triangle loop diagrams to the dipionic transition processes of the $X(3872)$ and its heavy quark flavor/spin symmetry partners is expected to be suppressed relative to the box diagrams [60–62]. In Ref. [60], based on a power counting scheme in heavy hadron chiral perturbation theory (HHχPT), the contributions of the triangle diagrams to the decay widths were estimated to be 1C3 magnitudes smaller than the box diagram contributions for $X_b \to \pi\pi\chi_{bJ}$. Similar conclusions were also drawn in the study of dipionic transitions of X_2 in Ref. [61] by using power counting rule, where the ratio of triangle diagrams and box diagrams is of order $O(0.1)$, although the power counting somewhat overestimates the suppression on the triangle loops for the $X_2 \to \pi\pi\chi_{cJ}$. The dipionic transitions from $X(3872)$ to η_c were studied in Ref. [62] using an effective Lagrangian approach, and the numerical results reveal that the decay width from the triangle diagrams is one order of magnitude smaller than that from box diagrams.

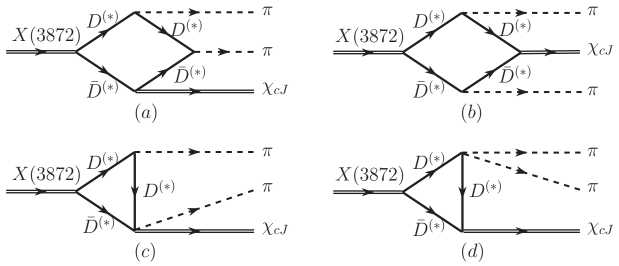

FIG. 1: Box [(a) and (b)] and triangle [(c) and (d)] diagrams contributing to the dipionic transitions from $X(3872)$ to χ_{cJ}.

In Ref. [37], we investigated the isospin-breaking in the hidden charm decay processes, $X(3872) \to \rho(\omega)J/\psi$ and $X(3872) \to \pi^0\chi_{cJ}$, with triangle loop mechanism and we found that isospin symmetry breaking stems from two aspects, which are the mass difference between charged and neutral charm mesons in the meson loop, and the different fraction of the charged and neutral components in the molecular states. In the present work, we study dipion transition processes $X(3872) \to \pi\pi\chi_{cJ}(J = 0, 1, 2)$ in HHχPT by considering box intermediate meson-loop (IML) contributions. This allows us to make model-independent predictions and provide quantitative estimates of different contributions based on the power counting. Under the molecular picture of $X(3872)$, we calculate the relative decay rates to different final states. These ratios serve as critical tests of the molecular interpretation, as heavy quark symmetry constrains their expected values.

The paper is organized as follows. In Sec. II, we present the details of the theoretical framework adopted in the present estimations. Numerical results and the relevant discussions are given in Sec. III, with conclusions summarized in Sec. IV.

II. THEORETICAL FRAMEWORK

A. Effective Lagrangians

The sketch diagrams contributing to the dipion decay processes $X(3872) \to \pi\pi\chi_{cJ}$, $(J = 0, 1, 2)$ are presented in Fig. 1, where diagrams (a)-(b) and (c)-(d) are box and triangle diagrams, respectively. Following Ref. [60], we estimate the relative contributions of box and triangle diagrams using NREFT power counting rule [63, 64]. In this framework, the momentum, nonrelativistic energy, integral measure, and heavy meson propagator count as v, v^2, v^5, and $1/v^2$, respectively. The S-wave vertices are velocity-independent, while P-wave vertices scale as either v or external momentum. As for Figs. 1(a) and 1(b), the vertices $XD\bar{D}^*/XD^*\bar{D}$ and $\chi_{cJ}D^{(*)}\bar{D}^{(*)}$ are in S-wave (scaling $\sim$ 1). The $D^*D^{(*)}\pi$ and $\chi_{cJ}D^{(*)}\bar{D}^{(*)}\pi$ vertices have P-wave couplings, introducing a factor $\vec{q}$ to the amplitudes, where $\vec{q}$ is the pion momentum. Besides, the four interaction vertices $D^{(*)}D^{(*)}\pi\pi$ is proportional to the square of the energy of the pion. As a result, the amplitude corresponding to Figs. 1(a) and 1(b) scales as $v^5\vec{q}^2/(v^2)^4 = \vec{q}^2/v^3$, and the amplitude related to Figs. 1(c) and 1(d) scales as $v^5\vec{q}^2/(v^2)^3 = \vec{q}^2/v$. The ratio of the amplitude from box and triangle diagrams can be roughly estimated to be $1/v^2$, where $v \ll 1$ since it is the typical velocity of the nonrelativistic intermediate mesons. Consequently, the contribution from box diagrams to the dipionic transitions from $X(3872)$ to χ_{cJ} is much larger than that from triangle diagrams.

The power counting analysis indicates that box diagrams dominate the dipionic transitions $X(3872) \to \pi\pi\chi_{cJ}$. We notice that the authors in Ref. [53] have studied the decays $X(3872) \to \pi\pi\chi_{cJ}$ by calculating the box diagrams via a phenomenological Lagrangian approach. However, they only consider the coupling of the $X(3872)$ with neutral component. In the following, we present the relevant effective Lagrangians associated with the box diagram calculations. The $X(3872)$ is assumed as an S-wave molecular state with the quantum numbers of $J^{PC} = 1^{++}$. As a pure hadronic molecule, the wave function of the $X(3872)$ can be written as

$$|X(3872)\rangle = \frac{\cos\theta}{\sqrt{2}}|D^{*0}\bar{D}^0 + D^0\bar{D}^{*0}\rangle + \frac{\sin\theta}{\sqrt{2}}|D^{*+}D^- + D^+D^{*-}\rangle, \quad (4)$$

where θ is the mixing angle describing the proportion of neutral and charged constituents.

The coupling of the $X(3872)$ to a pair of charmed and anticharmed mesons is described by effective Lagrangian

$$\mathcal{L}_X = \frac{g_n}{\sqrt{2}}X_i^\dagger(D^{*0i}\bar{D}^0 + D^0\bar{D}^{*0i}) + \frac{g_c}{\sqrt{2}}X_i^\dagger(D^{*+i}D^- + D^+D^{*-i}), \quad (5)$$

where $g_n = |g^n_{\rm NR}|\cos\theta$ and $g_c = |g^c_{\rm NR}|\sin\theta$ are the coupling constants of the $X(3872)$ with its neutral and charged components, respectively.

The pionic couplings to heavy mesons are constrained by chiral symmetry. For the S-wave heavy mesons, the leading order Lagrangian in heavy meson chiral perturbation theory is [65, 66]

$$\begin{aligned}\mathcal{L}_\pi &= -\frac{g}{2}\,{\rm Tr}[H_a^\dagger H_b\vec{\sigma}\cdot\vec{u}_{ba}] \\ &= \frac{\sqrt{2}g}{F}(i\epsilon^{ijk}V_a^{i\dagger}V_b^j\partial^k\phi_{ba} + V_a^{i\dagger}P_b\partial^i\phi_{ba} + P_a^\dagger V_b^i\partial^i\phi_{ba}),\end{aligned} \quad (6)$$

where the axial current is $\vec{u} = -\sqrt{2}\vec{\partial}\phi/F_\pi + \mathcal{O}(\phi^3)$. Charmed mesons with $s_l^P = 1/2^+$ form a spin multiplet, which is written as $H_a = \vec{V}_a\cdot\vec{\sigma} + P_a$ in two-component notation [66]. Here, F_π is the pion decay constant in the chiral limit, and

$$\phi = \begin{pmatrix}\pi^0/\sqrt{2} & \pi^+ \\ \pi^- & -\pi^0/\sqrt{2}\end{pmatrix}$$

collects the pion fields.

The coupling of the P-wave charmonia χ_{cJ} to a pair of charmed and anticharmed mesons is described as [28, 67]

$$\begin{aligned}\mathcal{L}_\chi &= i\frac{g_\chi}{2}{\rm Tr}[\chi^{\dagger i}H_a\sigma^i\bar{H}_a] + {\rm H.c.} \\ &= i2g_\chi\chi_{c2}^{\dagger ij}V_a^i\bar{V}_a^j + \sqrt{2}g_\chi\chi_{c1}^{\dagger i}(V_a^i\bar{P}_a + P_a\bar{V}_a^i) \\ &\quad + \frac{i}{\sqrt{3}}g_\chi\chi_{c0}^\dagger(\vec{V}_a\cdot\vec{\bar{V}}_a + 3P_a\bar{P}_a) + {\rm H.c.}\,,\end{aligned} \quad (7)$$

where χ denotes the field for the P-wave charmonia,

$$\chi^i = \sigma^j\left(-\chi_{c2}^{ij} - \frac{1}{\sqrt{2}}\epsilon^{ijk}\chi_{c1}^k + \frac{1}{\sqrt{3}}\delta^{ij}\chi_{c0}\right) + h_c^i. \quad (8)$$

B. Decay amplitudes

The relevant kinematics we used for calculations are explicitly indicated in Fig. 3. With the Lagrangians in Eqs. (5)-(7), the decay amplitudes for the $X(3872) \to \pi^0\pi^0\chi_{cJ}$ read as

$$\begin{aligned}\mathcal{M}_{\pi^0\pi^0\chi_{c0}} &= \sqrt{\frac{2}{3}}\frac{1}{F_\pi^2}g^2g_1q_1^iq_2^j\varepsilon^k(p)\epsilon_{ijk} \\ &\times\Big[g_n\Big(I_1(D^0,\bar{D}^{*0},\bar{D}^{*0},D^{*0}) + 3I_1(D^{*0},\bar{D}^0,\bar{D}^0,D^{*0}) \\ &-3I_1'(D^{*0},\bar{D}^0,\bar{D}^0,D^{*0}) - I_1'(D^0,\bar{D}^{*0},\bar{D}^{*0},D^{*0}) \\ &+I_2(D^{*0},\bar{D}^0,\bar{D}^{*0},D^{*0}) - I_2(D^0,\bar{D}^{*0},\bar{D}^{*0},D^{*0})\Big) \\ &+g_c\Big(I_1(D^+,D^{*-},D^{*-},D^{*+}) + 3I_1(D^{*+},D^-,D^-,D^{*+}) \\ &-3I_1'(D^{*+},D^-,D^-,D^{*+}) - I_1'(D^+,D^{*-},D^{*-},D^{*+}) \\ &+I_2(D^{*+},D^-,D^{*-},D^{*+}) - I_2(D^+,D^{*-},D^{*-},D^{*+})\Big)\Big],\end{aligned} \quad (9)$$

$$\begin{aligned}\mathcal{M}_{\pi^0\pi^0\chi_{c1}} &= \frac{2}{F_\pi^2}g^2g_1\Big\{\vec{q}_2\cdot\vec{\varepsilon}(p)\vec{q}_1\cdot\vec{\varepsilon}(q_3)\times \\ &\Big[g_n\Big(I_1(D^{*0},\bar{D}^0,D^{*0},D^{*0}) - I_1'(D^{*0},\bar{D}^0,\bar{D}^{*0},D^0) \\ &-I_2(D^0,\bar{D}^{*0},D^0,D^{*0})\Big) + g_c\Big(I_1(D^{*+},D^-,D^{*+},D^{*+}) \\ &-I_1'(D^{*+},D^-,D^{*-},D^+) - I_2(D^+,D^{*-},D^-,D^{*+})\Big)\Big] \\ &+\vec{q}_1\cdot\vec{\varepsilon}(p)\vec{q}_2\cdot\vec{\varepsilon}(q_3)\times \\ &\Big[g_n\Big(-I_1(D^{*0},\bar{D}^0,\bar{D}^{*0},D^0) + I_1'(D^{*0},\bar{D}^0,D^{*0},D^{*0}) \\ &-I_2(D^{*0},\bar{D}^0,\bar{D}^{*0},D^0)\Big) + g_c\Big(-I_1(D^{*+},D^-,D^{*-},D^+) \\ &+I_1'(D^{*+},D^-,D^{*+},D^{*+}) - I_2(D^{*+},D^-,D^{*-},D^+)\Big)\Big] \\ &+\vec{q}_1\cdot\vec{q}_2\vec{\varepsilon}(p)\cdot\vec{\varepsilon}(q_3)\times \\ &\Big[g_n\Big(-I_1(D^{*0},\bar{D}^0,D^{*0},D^{*0}) - I_1(D^0,\bar{D}^{*0},D^0,D^{*0}) \\ &-I_1'(D^0,\bar{D}^{*0},D^0,D^{*0}) - I_1'(D^{*0},\bar{D}^0,D^{*0},D^{*0})\Big) \\ &+g_c\Big(-I_1(D^{*+},D^-,D^{*+},D^{*+}) - I_1(D^+,D^{*-},D^-,D^{*+}) \\ &-I_1'(D^{*+},D^-,D^{*+},D^{*+}) - I_1'(D^+,D^{*-},D^-,D^{*+})\Big)\Big]\Big\},\end{aligned} \quad (10)$$

and

$$\mathcal{M}_{\pi^0\pi^0\chi_{c2}} = -\frac{2\sqrt{2}}{F_\pi^2} g^2 g_1 \Big\{\epsilon_{ikl} q_1^i q_2^j \varepsilon^k(p)\varepsilon_j^l(q_3) \\ \Big[g_n I_2(D^{*0},\bar{D}^0,\bar{D}^{*0},D^{*0}) + g_c I_2(D^{*+},D^-,D^{*-},D^{*+})\Big] \\ +\epsilon_{jkl} q_1^i q_2^j \varepsilon^k(p)\varepsilon_i^l(q_3)\Big[g_n I_2(D^0,\bar{D}^{*0},D^{*0},D^{*0}) \\ +g_c I_2(D^+,D^{*-},D^{*-},D^{*+})\Big] + \epsilon_{jkl} q_1^j q_2^k \varepsilon^i(p)\varepsilon_i^l(q_3) \\ \Big[g_n\Big(-I_1(D^0,\bar{D}^{*0},D^{*0},D^{*0}) + I_1'(D^0,\bar{D}^{*0},D^{*0},D^{*0})\Big) \\ g_c\Big(-I_1(D^+,D^{*-},D^{*-},D^{*+}) + I_1'(D^+,D^{*-},D^{*-},D^{*+})\Big]\Big\}, \quad (11)$$

where $\varepsilon^i(p)$ and $\varepsilon^i(q_3)$ are the polarization vector of $X(3872)$ and χ_{c1}, respectively. $\varepsilon^{ij}(q_3)$ is the symmetric polarization tensor for the χ_{c2}. I_1, I_1' and I_2 are the four point scalar integral, where the first particle in each square bracket denotes the top left intermediate charmed meson in the corresponding diagram, and the other intermediate charmed mesons in the same diagram are listed in the square bracket in counterclockwise order along the loop. The four point scalar integral I_1, I_1' and I_2 are given in Appendix A and the decay amplitudes of $X(3872) \to \pi^+\pi^-\chi_{cJ}$ are present in Appendix B. Using the amplitudes in Eqs. (9)-(11), the decay width of $X(3872) \to \pi\pi\chi_{cJ}$ can be obtained by performing three-body phase space integral. The decay width of $X(3872) \to \pi\pi\chi_{cJ}$ is

$$\Gamma_{X(3872)\to\pi\pi\chi_{cJ}} = \frac{1}{2J+1}\frac{1}{2S\,m_X^2}\frac{N^2}{32\pi^3}\int_0^\pi \int_{2m_\pi}^{m_X-m_{\chi_{cJ}}} \times \vec{q}_1^{\,*}\vec{q}_3 \sin\theta_1^* |\mathcal{M}_{\pi\pi\chi_{cJ}}|^2 dm_{12} d\theta_1^*\,, \quad (12)$$

where $N = \sqrt{m_X m_{\chi_{cJ}}}$ accounts for the nonrelativistic normalization. Similar factors for the intermediate charmed mesons have been absorbed in the definition of the loop function. J is the total spin of the initial particle. The symmetry factor S is taken to be 2 for $X(3872) \to \pi^0\pi^0\chi_{cJ}$ decays (considering identical $\pi^0\pi^0$ particles in the final states), and 1 for $X(3872) \to \pi^+\pi^-\chi_{cJ}$ decays. The $|\vec{q}_1^{\,*}|$ and $|\vec{q}_3|$ are the three-momenta of the outgoing π meson in the center of mass frame of the final $\pi\pi$ system and the outgoing χ_{cJ} meson in the $X(3872)$ rest frame, respectively. They are given by

$$|\vec{q}_1^{\,*}| = \frac{\lambda^{1/2}(m_{12}^2, m_1^2, m_2^2)}{2m_{12}},$$
$$|\vec{q}_3| = \frac{\lambda^{1/2}(m^2, m_{12}^2, m_3^2)}{2m}, \quad (13)$$

where $\lambda(x,y,z)$ is the K*ä*hlen or triangle function.

III. NUMERICAL RESULTS AND DISCUSSION

Before estimating the partial widths of the considered processes, we first discuss the coupling constants involved in our calculations. As a molecular state, the $X(3872)$ lies slightly below $D^*\bar{D}$ threshold. The effective coupling constant $g_{\rm NR}$, indicating the coupling between $X(3872)$ and its components, is [68, 69]

$$g_{\rm NR}^2 = \lambda^2 \frac{16\pi}{\mu}\sqrt{\frac{2\epsilon}{\mu}}[1 + O(\sqrt{2\mu\epsilon r})], \quad (14)$$

where $\epsilon = m_D + m_{D^*} - M_X$ denotes the binding energy of the $X(3872)$ and $\mu = m_D m_{D^*}/(m_D + m_{D^*})$ is the reduced mass. The force range is estimated as $r^{-1} \sim \sqrt{2\mu\epsilon_{th}}$, where μ is the reduced mass and ϵ_{th} is the mass difference between the relevant threshold and the nearest one. For the $X(3872)$, this is given by $(m_{D^{*+}} + m_{D^+}) - (m_{D^{*0}} + m_{D^0})$. λ^2 gives the probability of finding the molecular component in the physical state. Since the $X(3872)$ is treated as a pure molecular state, $\lambda^2 = 1$. Taking $m_X = 3871.64$ MeV, the effective couplings are determined as $|g_{\rm NR}^n| = 0.73 \pm 0.34 \pm 0.08\ {\rm GeV}^{-1/2}$ and $|g_{\rm NR}^c| = 2.60 \pm 0.03 \pm 1.00\ {\rm GeV}^{-1/2}$, respectively, where the first uncertainty originates from the binding energies, and the second stems from the approximate nature of Eq. (14).

The coupling g_χ can be derived from vector meson dominance [67, 70], given by $g_\chi = -\sqrt{m_{\chi_{c0}}/6}/f_{\chi_{c0}}$. With $m_{\chi_{c0}} = 3417.71$ MeV and $f_{\chi_{c0}} = 510$ MeV, we obtain $g_\chi = -1.48\ {\rm GeV}^{-1/2}$. However, the VMD model may overestimate the coupling g_χ in both the charm sector [71] and the bottom sector [72]. Utilizing recent precise determinations of the pole position and the isospin breaking properties of the $X(3872)$, the upper bound of g_χ^2 is $0.28^{+1.36}_{-0.14}\ {\rm GeV}^{-1}$ [71]. Following Ref. [71], we adopt a value of $g_\chi = 0.53^{+1.82}_{-0.19}\ {\rm GeV}^{-1/2}$. For the pionic couplings to heavy mesons, we use $g = 0.79 \pm 0.13$ in this work, which is extracted from a tree level calculation of the D^{*+} width.

In Table I, we present the branching ratios for $X(3872) \to \pi\pi\chi_{cJ}$ as functions of the mixing angle θ, considering representative values $\theta = 0, \pi/2, \pi/4$, and $\pi/2$. The dominant uncertainties in our model originate from the couplings at the four vertices of the box diagrams, specifically, the errors of the coupling constants $g_{NR}^{n/c}$, g, and g_χ. The angles $\theta = 0$ and $\theta = \pi/2$ denote the $X(3872)$ as a pure $D^0\bar{D}^{*0} + c.c$ and a pure $D^+D^{*-} + c.c$ molecular state, respectively. The angle $\theta = \pi/4$ represents an equal proportion of neutral and charged molecular components, while $\theta = \pi/12$ approximately stands for an isospin singlet state with predominantly neutral constituents. The orders of magnitude for the branching fractions of $X(3872) \to \pi\pi\chi_{cJ}$ with $J = 0$, 1, and 2 are 10^{-4}, 10^{-3}, and 10^{-5}, respectively. The channels $\pi\pi\chi_{c0/1}$ achieve the maximum at $\theta = \pi/4$, while channel $\pi\pi\chi_{c2}$ increases monotonically from $\theta = 0$ to $\pi/2$. It is interesting to see that the channel $\pi^+\pi^-\chi_{c1}$ seems more sensitive to the mixing angle θ than other channels, reflecting that the decay $X(3872) \to \pi^+\pi^-\chi_{c1}$ is sensitive to the proportion of neutral and charged molecular components in the $X(3872)$.

From Eq. (2), one can find that the upper limits of the branching ratios of $X(3872) \to \pi^0\pi^0\chi_{c0}$ and $X(3872) \to \pi^+\pi^-\chi_{c0}$ are 7.31% and 2.41%, respectively. Our results indicate that the corresponding branching ratios are $(0.17^{+0.83}_{-0.15} \sim 0.90^{+4.39}_{-0.75}) \times 10^{-4}$ and $(0.25^{+1.23}_{-0.23} \sim 1.40^{+6.86}_{-1.17}) \times 10^{-4}$, respectively, which are two orders of magnitude smaller than the upper limits measured by the BESIII Collaboration. In Ref. [28],

TABLE I: The branching ratios of $X(3872) \to \pi\pi\chi_{cJ}$ ($J = 0, 1, 2$) in the present work for different θ values (in units of 10^{-4}, 10^{-3}, and 10^{-5} for J = 0, 1, and 2, respectively). The ratio $\mathcal{R}$ is defined in Eq. (15), which is in units of 10^{-3}, 10^{-2}, and 10^{-4} for J = 0, 1, and 2, respectively. The branching fractions estimated by other theoretical studies [28, 31, 53, 59] and experimental measurements [56–58] are also listed for comparison.

Channel	Present work					Ref. [28]	Ref. [31]	Ref. [53]	Ref. [59]	Exp. data [56–58]
	0	$\pi/12$	$\pi/4$	$\pi/2$	$\mathcal{R}$					
$\pi^0\pi^0\chi_{c0}$	$0.17^{+0.83}_{-0.15}$	$0.41^{+1.99}_{-0.35}$	$0.90^{+4.39}_{-0.75}$	$0.86^{+4.20}_{-0.69}$	$0.40^{+1.93}_{-0.37} \sim 2.09^{+10.2}_{-1.87}$	1.4×10^{-6}	...	0.79×10^{-4}	...	$< 7.31\%$
$\pi^+\pi^-\chi_{c0}$	$0.25^{+1.23}_{-0.23}$	$0.62^{+3.03}_{-0.54}$	$1.40^{+6.86}_{-1.17}$	$1.38^{+6.75}_{-1.11}$	$0.58^{+2.87}_{-0.57} \sim 3.26^{+16.0}_{-2.92}$	2.8×10^{-6}	...	...	...	$< 2.41\%$
$\pi^0\pi^0\chi_{c1}$	$0.57^{+2.79}_{-0.51}$	$1.18^{+5.79}_{-1.03}$	$2.30^{+11.3}_{-1.94}$	$1.97^{+9.64}_{-1.59}$	$1.33^{+6.50}_{-1.26} \sim 5.35^{+26.3}_{-4.84}$	2.3%	1.1×10^{-4}	0.92×10^{-3}	$(0.77 \sim 1.63) \times 10^{-4}$	$< 4.73\%$
$\pi^+\pi^-\chi_{c1}$	$0.57^{+2.80}_{-0.51}$	$1.37^{+6.71}_{-1.19}$	$3.02^{+14.8}_{-2.53}$	$2.90^{+14.2}_{-2.34}$	$1.33^{+6.53}_{-1.26} \sim 7.02^{+34.5}_{-6.31}$	$\mathcal{O}(10^{-5})$	...	...	$(0.86 \sim 1.77) \times 10^{-4}$	$< 0.77\%$
$\pi^0\pi^0\chi_{c2}$	$0.15^{+0.76}_{-0.14}$	$0.42^{+2.05}_{-0.36}$	$1.01^{+4.96}_{-0.84}$	$1.06^{+5.20}_{-0.86}$	$0.35^{+1.77}_{-0.34} \sim 2.47^{+12.1}_{-2.16}$	3.9×10^{-7}	...	2.55×10^{-5}	...	$< 2.15\%$
$\pi^+\pi^-\chi_{c2}$	$0.13^{+0.62}_{-0.11}$	$0.35^{+1.73}_{-0.30}$	$0.88^{+4.28}_{-0.73}$	$0.93^{+4.58}_{-0.75}$	$0.30^{+1.46}_{-0.27} \sim 2.16^{+10.7}_{-1.88}$	7.8×10^{-7}	...	...	...	-

the ratio $\mathcal{B}[X(3872) \to \pi^0\pi^0\chi_{c0}]/\mathcal{B}[X(3872) \to \pi^0\chi_{c0}]$ is estimated as 9.1×10^{-6} at leading order (LO) in χPT. Given the upper limit $\mathcal{B}[X(3872) \to \pi^0\chi_{c0}] = 15.5\%$ [56], the upper limits are $\mathcal{B}[X(3872) \to \pi^0\pi^0\chi_{c0}] = 1.4 \times 10^{-6}$ and $\mathcal{B}[X(3872) \to \pi^+\pi^-\chi_{c0}] \leq 2.8 \times 10^{-6}$ under isospin symmetry [28], which are about four orders and two orders of magnitude smaller than the BESIII upper limits and our present estimations, respectively. In addition, in Ref. [53], the branching ratios for $X(3872) \to \pi^0\pi^0\chi_{cJ}$ are estimated to be 0.79×10^{-4}, 0.92×10^{-3}, and 2.55×10^{-5} for J = 0, 1, and 2, respectively. This corresponds to the case of $\theta = 0$ in our work, and the values are mutually consistent.

As for the decay processes $X(3872) \to \pi\pi\chi_{c1}$, the upper limits of the branching ratios estimated from Eq. (3) are 4.73% and 0.77% for $X(3872) \to \pi^0\pi^0\chi_{c1}$ and $X(3872) \to \pi^+\pi^-\chi_{c1}$, respectively. Our results indicate that the branching ratios of $X(3872) \to \pi^0\pi^0\chi_{c1}$ and $X(3872) \to \pi^+\pi^-\chi_{c1}$ are $(0.57^{+2.79}_{-0.51} \sim 2.30^{+11.3}_{-1.94}) \times 10^{-3}$ and $(0.57^{+2.80}_{-0.51} \sim 3.02^{+14.8}_{-2.53}) \times 10^{-3}$, respectively. The branching ratio for $X(3872) \to \pi^0\pi^0\chi_{c1}$ estimated in the present work is one order of magnitude smaller than the upper limits reported by the BESIII Collaboration. As for the processes $X(3872) \to \pi^+\pi^-\chi_{c1}$, our predictions for the branching ratio is compatible with the BESIII Collaboration's upper limits. In Ref. [28], using $\mathcal{B}[X(3872) \to \pi^0\chi_{c1}] = 3.8\%$ [54], $\mathcal{B}[X(3872) \to \pi^0\pi^0\chi_{c1}]$ was estimated to be 2.32%, while $\mathcal{B}[X(3872) \to \pi^+\pi^-\chi_{c1}] = \mathcal{O}(10^{-5})$ [28]. A later study in Ref. [31] revised $\mathcal{B}[X(3872) \to \pi^0\pi^0\chi_{c1}]$ to be 1.1×10^{-4} through corrected treatment of infrared divergences. Moreover, in Ref. [59], the branching ratios of $X(3872) \to \pi^0\pi^0\chi_{c1}$ and $X(3872) \to \pi^+\pi^-\chi_{c1}$ were estimated to be $(0.8 \sim 1.7) \times 10^{-4}$, which is lower than our present estimations by $1 \sim 2$ order of magnitude and consistent with our powering counting analysis.

For the decay process $X(3872) \to \pi\pi\chi_{c2}$, the upper limit estimated from Eq. (3) is 2.15%. Our results indicate that the branching ratios of $X(3872) \to \pi^0\pi^0\chi_{c2}$ and $X(3872) \to \pi^+\pi^-\chi_{c2}$ are $(0.15^{+0.76}_{-0.14} \sim 1.06^{+5.20}_{-0.86}) \times 10^{-5}$ and $(0.13^{+0.62}_{-0.11} \sim 0.93^{+4.58}_{-0.75}) \times 10^{-5}$, respectively, which are three orders of magnitude lower than the upper limit measured from the BESIII Collaboration. Using $\mathcal{B}[X(3872) \to \pi^0\chi_{c2}] < 5\%$ [55], isospin symmetry yields upper limits of $\mathcal{B}[X(3872) \to \pi^0\pi^0\chi_{c2}] \lesssim 3.9 \times 10^{-7}$ and $\mathcal{B}[X(3872) \to \pi^+\pi^-\chi_{c2}] \lesssim 7.8 \times 10^{-7}$ [28], five orders of magnitude below BESIII measurements.

The ratios of $\mathcal{B}[X(3872) \to \pi\pi\chi_{cJ}]$ and $\mathcal{B}[X(3872) \to \pi^+\pi^- J/\psi]$ should be more accessible experimentally. Using $\mathcal{B}[X(3872) \to \pi^+\pi^- J/\psi] = (4.3 \pm 1.4)\%$ [55] and the branching ratios of $X(3872) \to \pi\pi\chi_{cJ}$ in Table I, the ratios,

$$\mathcal{R} = \frac{\mathcal{B}[X(3872) \to \pi\pi\chi_{cJ}]}{\mathcal{B}[X(3872) \to \pi^+\pi^- J/\psi]}, \tag{15}$$

are estimated and the values are listed in Table I. Experimental upper limits for the ratios $\mathcal{B}[X(3872) \to \pi\pi\chi_{cJ}]/\mathcal{B}[X(3872) \to \pi^+\pi^- J/\psi]$ are given in Eqs. (2)-(3), except for $\mathcal{B}[X(3872) \to \pi^+\pi^-\chi_{c2}]/\mathcal{B}[X(3872) \to \pi^+\pi^- J/\psi]$. Comparison with $\mathcal{R}$ from the present work shows that our results are lower than these experimental upper limits by $2 \sim 3$ orders of magnitude for $J = 0$ and 2. For $J = 1$, the predicted ratio $\mathcal{B}[X(3872) \to \pi^0\pi^0\chi_{c1}]/\mathcal{B}[X(3872) \to \pi^+\pi^- J/\psi]$ is an order of magnitude below the experimental upper limit, while $\mathcal{B}[X(3872) \to \pi^+\pi^-\chi_{c1}]/\mathcal{B}[X(3872) \to \pi^+\pi^- J/\psi]$ covers the experimental upper limit in the range of $\theta = 0 \sim \pi/2$. We therefore conclude that precision measurements of the decays $X(3872) \to \pi\pi\chi_{c1}$ are promising. Given that theoretical predictions lie $2 \sim 3$ orders of magnitude below current experimental upper limits, the decays $X(3872) \to \pi\pi\chi_{c0/2}$ require more data samples and more precise experimental studies.

Using the branching ratios in Table I, we can also estimate the ratios for $X(3872) \to \pi\pi\chi_{cJ}$ with different J. For this purpose, we define

$$R^n_{0/2} = \frac{\mathcal{B}[X(3872) \to \pi^0\pi^0\chi_{c0/2}]}{\mathcal{B}[X(3872) \to \pi^0\pi^0\chi_{c1}]},$$
$$R^c_{0/2} = \frac{\mathcal{B}[X(3872) \to \pi^+\pi^-\chi_{c0/2}]}{\mathcal{B}[X(3872) \to \pi^+\pi^-\chi_{c1}]}. \tag{16}$$

Our results indicate the ratios R^n_0, R^n_2, R^c_0 and R^c_2 are $(2.98^{+20.6}_{-3.75} \sim 3.91^{+27.1}_{-4.64}) \times 10^{-2}$, $(2.63^{+18.5}_{-3.40} \sim 4.61^{+32.0}_{-5.39}) \times 10^{-3}$,

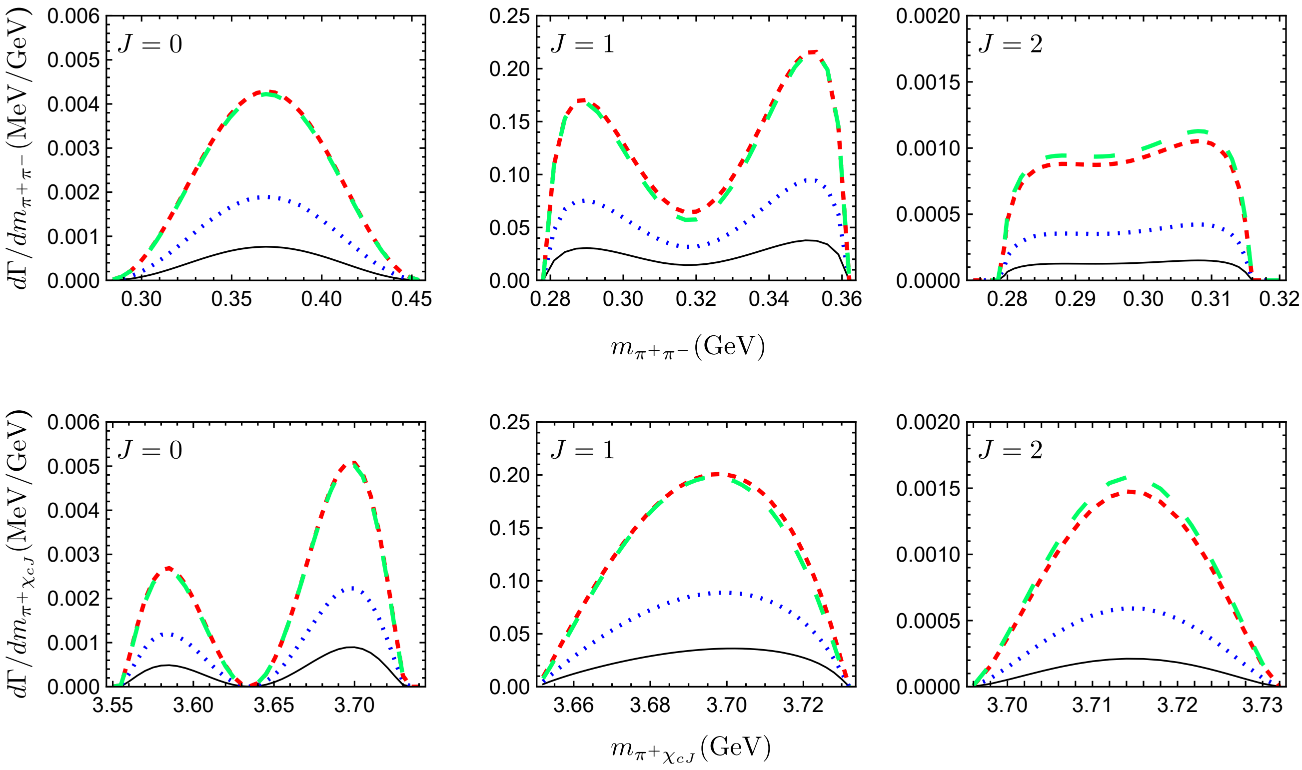

FIG. 2: Invariant mass distributions of $\pi^+\pi^-$ and $\pi^+\chi_{cJ}$ for the decays of $X(3872) \to \pi^+\pi^-\chi_{cJ}$, $(J = 0, 1, 2)$. The black, blue, red, and green lines correspond to $\theta = 0$, $\pi/12$, $\pi/4$, and $\pi/2$, respectively.

$(4.39^{+30.5}_{-5.63} \sim 4.64^{+32.1}_{-5.49}) \times 10^{-2}$, and $(2.28^{+15.6}_{-2.81} \sim 3.08^{+21.4}_{-3.58}) \times 10^{-3}$, respectively. The predicted ratios can be tested by future experiments. These measurements will help us better understand the molecular nature of the $X(3872)$ and constrain the mixing angle θ.

In Ref. [59], the ratio $\mathcal{B}[X(3872) \to \pi^+\pi^-\chi_{c1}]/\mathcal{B}[X(3872) \to \pi^0\pi^0\chi_{c1}]$ was determined as 1.1. This deviates from the expectation of 2 under exact isospin symmetry. In order to investigate the ratios of the considered decay processes with charged and neutral dipion, we define

$$R_J = \frac{\mathcal{B}[X(3872) \to \pi^+\pi^-\chi_{cJ}]}{\mathcal{B}[X(3872) \to \pi^0\pi^0\chi_{cJ}]}. \tag{17}$$

The ratio R_1 is estimated to be $1.00^{+6.93}_{-1.27} \sim 1.31^{+9.11}_{-1.56}$, consistent with the estimations in Ref. [59], which is $1.07 \sim 1.22$. Notably, $R_1 \approx 1.00$ at $\theta = 0$ implies strong isospin violation in $X(3872) \to \pi\pi\chi_{c1}$ transitions for a pure neutral molecular state. As θ increases from 0 to $\pi/2$, the ratios R_0 and R_2 are in the range of $1.47^{+10.2}_{-1.87} \sim 1.56^{+10.8}_{-1.84}$ and $0.87^{+6.03}_{-1.09} \sim 0.88^{+6.10}_{-1.00}$, respectively. Experimental measurement of R_J could constrain θ and elucidate the $X(3872)$ molecular structure. Although the ratios R_J deviate from the isospin-symmetric expectation of 2, the degree of deviation differs for $J = 0, 1, 2$. R_0 and R_1 are closer to 2 and 1, respectively, and R_2 small than 1, indicating that the degree of isospin-symmetry violation follows the ordering $X(3872) \to \pi\pi\chi_{c2} > X(3872) \to \pi\pi\chi_{c1} > X(3872) \to \pi\pi\chi_{c0}$.

The ratios R_J probe the isospin structure of the $X(3872)$ molecular state, which is a superposition of neutral $(|D^{*0}\bar{D}^0 + \bar{D}^0 D^{*0}\rangle)$ and charged $(|D^{*+}D^- + D^+D^{*-}\rangle)$ components parameterized by a mixing angle θ. These ratios provide crucial insight into the isospin configuration of $X(3872)$. The ratios R_0, R_1 and R_2 vary with θ, demonstrating how isospin mixing influences decay patterns. The ratios R_J exhibit minimal θ-dependence, increasing slightly with θ. This indicates that the charged components enhance the decays $X(3872) \to \pi^+\pi^-\chi_{cJ}$. Deviations of R_J from 2 reveal significant isospin-symmetry violation in $X(3872) \to \pi\pi\chi_{cJ}$ decays. When masses of the isospin-triplet $D^{(*)}$ and π states are set equal, i.e., $m_{D^{(*)+}} = m_{D^{(*)0}}$ and $m_{\pi^\pm} = m_{\pi^0}$, the ratios R_J are equal to 2 at $\theta = \pi/12$. Thus, isospin breaking in $X(3872) \to \pi\pi\chi_{cJ}$ originates from the mass difference between the u and d quarks.

In addition to calculating the branching ratios for the decays $X(3872) \to \pi^+\pi^-\chi_{cJ}$, $(J = 0, 1, 2)$, we have also analyzed the invariant mass distributions of both the $\pi^+\pi^-$ system and the $\pi^+\chi_{cJ}$ combination, as shown in Figs. 2. For $J = 0$, the distribution of $d\Gamma_{X\to\pi^+\pi^-\chi_{c0}}/dm_{\pi^+\pi^-}$ exhibits a broad single bump, peaking at approximately 0.369 GeV. Interestingly, we find a double-bump structure in the $d\Gamma_{X\to\pi^+\pi^-\chi_{c0}}/dm_{\pi^+\chi_{c0}}$ distribution. We suggest experimental studies of the $\pi^+\chi_{c0}$ invariant mass spectrum in the decay $X(3872) \to \pi^+\pi^-\chi_{c0}$ around 3.585 and 3.7 GeV. For $J = 1$, a double-bump structure, which peaks at 0.29 and 0.35 GeV, emerges in the $d\Gamma_{X\to\pi^+\pi^-\chi_{c1}}/dm_{\pi^+\pi^-}$ distribution. The double-bump structure, resulting from loop diagrams, can be recognized as evidence for the hadronic molecular nature of the $X(3872)$, and has been proposed as an observable to distinguish the hadronic molecular and the compact state pictures of the $D_{s1}(2460)$ [73]. The distributions of $d\Gamma_{X\to\pi^+\pi^-\chi_{c1}}/dm_{\pi^+\chi_{c1}}$ exhibits a broad single bump and peaking at 3.702 GeV ^{2}. For $J=2$, the distribution of $d\Gamma_{X\to\pi^+\pi^-\chi_{c2}}/dm_{\pi^+\pi^-}$ shows a much broader bump. The distribution of $d\Gamma_{X\to\pi^+\pi^-\chi_{c2}}/dm_{\pi^+\chi_{c2}}$ shows a broad single bump and peaking at 3.714 GeV.

IV. SUMMARY

The $X(3872)$, discovered in 2003, challenges conventional quark models due to its proximity to the $D^0\bar{D}^{*0}$ threshold, suggesting a dominant molecular structure. Its decays exhibit significant isospin violation, evidenced by comparable branching ratios $\mathcal{B}(X\to\rho^0 J/\psi)\sim\mathcal{B}(X\to\omega J/\psi)$. Recent BESIII measurements of $\mathcal{B}(X\to\pi^0\chi_{c1})\sim 3.8\%$ and upper limits for dipionic transitions (e.g., $\mathcal{B}(X\to\pi^+\pi^-\chi_{c1})<0.77\%$) motivate theoretical studies of dipionic transitions $X(3872)\to\pi\pi\chi_{cJ}$ ($J=0,1,2$) as probes of its internal structure.

Using heavy hadron chiral perturbation theory (HHχPT), we investigate $X(3872)\to\pi\pi\chi_{cJ}$ by treating the $X(3872)$ as a superposition of neutral and charged molecular components with a mixing angle. We employ NREFT power counting rules to analyze box and triangle diagrams and find that box diagrams dominate the dipionic transitions $X(3872)\to\pi\pi\chi_{cJ}$. The branching ratios of $X(3872)\to\pi\pi\chi_{cJ}$ with $J=0$, 1, and 2 are estimated to be of order 10^{-4}, 10^{-3} and 10^{-5}, respectively. The ratios $\mathcal{B}[X\to\pi\pi\chi_{cJ}]/\mathcal{B}[X\to\pi^+\pi^- J/\psi]$ are predicted, and the results reveal that $X(3872)\to\pi\pi\chi_{c1}$ decays are prime targets for the BESIII and Belle II Collaborations, while the $\chi_{c0/2}$ channels require higher precision.

The ratios $\mathcal{B}[X(3872)\to\pi\pi\chi_{c0/2}]/\mathcal{B}[X(3872)\to\pi\pi\chi_{c1}]$ and $\mathcal{B}[X(3872)\to\pi^+\pi^-\chi_{cJ}]/\mathcal{B}[X(3872)\to\pi^0\pi^0\chi_{cJ}]$ are also predicted. The latter ratios deviate from isospin-symmetric expectations. Specifically, the ratios are $1.47^{+10.2}_{-1.87}\sim 1.56^{+10.8}_{-1.84}$, $1.00^{+6.93}_{-1.27}\sim 1.31^{+9.11}_{-1.56}$, and $0.87^{+6.03}_{-1.09}\sim 0.88^{+6.10}_{-1.00}$ for $J=0$, 1, and 2, respectively, showing different degrees of isospin violation and the degree of isospin-symmetry violation follows the order $X(3872)\to\pi\pi\chi_{c2}>X(3872)\to\pi\pi\chi_{c1}>X(3872)\to\pi\pi\chi_{c0}$. Future measurements of R_J will constrain the mixing angle θ, resolving the neutral/charged mixing fraction and refining molecular models. The invariant mass distributions of $\pi^+\pi^-$ and $\pi^+\chi_{cJ}$ for the decay of $X(3872)\to\pi^+\pi^-\chi_{cJ}$ are studied. We find a double-bump structure in the $d\Gamma_{X\to\pi^+\pi^-\chi_{c1}}/dm_{\pi^+\pi^-}$ distribution and the $d\Gamma_{X\to\pi^+\pi^-\chi_{c0}}/dm_{\pi^+\chi_{c0}}$ distribution, which could be tested by the future experiments.

ACKNOWLEDGMENTS

Qi Wu thanks Zhao-Sai Jia for useful discussions. This work is supported by the National Natural Science Foundation of China under the Grant Nos. 12175037, 12335001, 12475081, 12105153, and 12405093, as well as supported, in part, by National Key Research and Development Program under Grant No.2024YFA1610503 and 2024YFA1610504. It is also supported by Taishan Scholar Project of Shandong Province under Grant No. tsqn202103062 and by the Natural Science Foundation of Shandong Province under Grant Nos. ZR2025MS04 and ZR2022ZD26.

Appendix A: Decay amplitudes

The decay amplitudes for the $X(3872)\to\pi^+\pi^-\chi_{cJ}$ read

$$\begin{aligned}\mathcal{M}_{\pi^+\pi^-\chi_{c0}} = &\sqrt{\frac{2}{3}}\frac{1}{F_\pi^2}g^2 g_1 q_1^i q_2^j \varepsilon^k(p)\epsilon_{ijk}\times\Big[g_n\Big(I_1(\bar{D}^0,D^{*0},D^{*0},D^{*-})+3I_1(\bar{D}^{*0},D^0,D^0,D^{*-})\\&-3I_1'(D^{*0},\bar{D}^0,\bar{D}^0,D^{*+})-I_1'(D^0,\bar{D}^{*0},\bar{D}^{*0},D^{*+})+I_2(\bar{D}^{*0},D^0,D^{*+},D^{*-})-I_2(\bar{D}^0,D^{*0},D^{*+},D^{*-})\Big)\\&+g_c\Big(I_1(D^+,D^{*-},D^{*-},D^{*0})+3I_1(D^{*+},D^-,D^-,D^{*0})-3I_1'(D^{*-},D^+,D^+,\bar{D}^{*0})-I_1'(D^-,D^{*+},D^{*+},\bar{D}^{*0})\\&+I_2(D^{*+},D^-,\bar{D}^{*0},D^{*0})-I_2(D^+,D^{*-},\bar{D}^{*0},D^{*0})\Big)\Big],\end{aligned}\tag{A1}$$

$$\begin{aligned}\mathcal{M}_{\pi^+\pi^-\chi_{c1}} = &\frac{2}{F_\pi^2}g^2 g_1\Big\{\vec{q}_2\cdot\vec{\varepsilon}(p)\vec{q}_1\cdot\vec{\varepsilon}(q_3)\times\Big[g_n\Big(I_1(\bar{D}^{*0},D^0,D^{*0},D^{*-})-I_1'(D^{*0},\bar{D}^0,\bar{D}^{*0},D^+)-I_2(\bar{D}^0,D^{*0},D^+,D^{*-})\Big)\\&+g_c\Big(I_1(D^{*+},D^-,D^{*-},D^{*0})-I_1'(D^{*-},D^+,D^{*+},\bar{D}^0)-I_2(D^+,D^{*-},\bar{D}^0,D^{*0})\Big)\Big]\\&+\vec{q}_1\cdot\vec{\varepsilon}(p)\vec{q}_2\cdot\vec{\varepsilon}(q_3)\times\Big[g_n\Big(-I_1(\bar{D}^{*0},D^0,D^{*0},D^-)+I_1'(D^{*0},\bar{D}^0,\bar{D}^{*0},D^{*+})-I_2(\bar{D}^{*0},D^0,D^{*+},D^-)\Big)\\&+g_c\Big(-I_1(D^{*+},D^-,D^{*-},D^0)+I_1'(D^{*-},D^+,D^{*+},\bar{D}^{*0})-I_2(D^{*+},D^-,\bar{D}^{*0},D^0)\Big)\Big]\\&+\vec{q}_1\cdot\vec{q}_2\vec{\varepsilon}(p)\cdot\vec{\varepsilon}(q_3)\times\Big[g_n\Big(-I_1(\bar{D}^0,D^{*0},D^0,D^{*-})-I_1(\bar{D}^{*0},D^0,D^{*0},D^{*-})-I_1'(D^0,\bar{D}^{*0},\bar{D}^0,D^{*+})-I_1'(D^{*0},\bar{D}^0,\bar{D}^{*0},D^{*+})\Big)\\&+g_c\Big(-I_1(D^{*+},D^-,D^{*-},D^{*0})-I_1(D^+,D^{*-},D^-,D^{*0})-I_1'(D^{*-},D^+,D^{*+},\bar{D}^{*0})-I_1'(D^-,D^{*+},D^+,\bar{D}^{*0})\Big)\Big]\Big\},\end{aligned}\tag{A2}$$

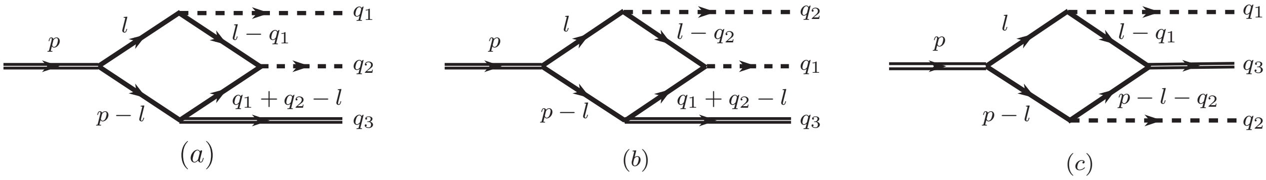

FIG. 3: Kinematics used for calculating 4-point integrals.

$$\begin{aligned}\mathcal{M}_{\pi^+\pi^-\chi_{c2}} = -\frac{2\sqrt{2}}{F_\pi^2} g^2 g_1 \Big\{ &\epsilon_{ikl} q_1^i q_2^j \varepsilon^k(p) \varepsilon_j^l(q_3) \Big[g_n I_2(\bar{D}^{*0}, D^0, D^{*+}, D^{*-}) + g_c I_2(D^{*+}, D^-, \bar{D}^{*0}, D^{*0}) \Big] \\ &+ \epsilon_{jkl} q_1^i q_2^j \varepsilon^k(p) \varepsilon_i^l(q_3) \Big[g_n I_2(\bar{D}^0, D^{*0}, D^{*+}, D^{*-}) + g_c I_2(D^+, D^{*-}, \bar{D}^{*0}, D^{*0}) \Big] + \epsilon_{jkl} q_1^j q_2^k \varepsilon^i(p) \varepsilon_i^l(q_3) \Big[g_n \Big(- I_1(\bar{D}^0, D^{*0}, D^{*0}, D^{*-}) \\ &+ I_1'(D^0, \bar{D}^{*0}, \bar{D}^{*0}, D^{*+}) \Big) + g_c \Big(- I_1(D^+, D^{*-}, D^{*-}, D^{*0}) + I_1'(D^-, D^{*+}, D^{*+}, \bar{D}^{*0}) \Big) \Big] \Big\}. \end{aligned} \tag{A3}$$

Appendix B: 4-point loop integrals

Following Refs. [60, 74], we present the analytical expression of scalar 4-point loop integrals. In the rest frame of the decay particle $p = (M, 0)$, they are written as

$$I_1[m_1, m_2, m_3, m_4] = \frac{-\mu_{12}\mu_{23}\mu_{24}}{2} \int \frac{d^3 l}{(2\pi)^3} \frac{1}{\left[\vec{l}^2 + c_{12} - i\epsilon\right] \left[\vec{l}^2 + 2\frac{\mu_{23}}{m_3}\vec{l}\cdot\vec{q}_3 + c_{23} - i\epsilon\right] \left[\vec{l}^2 - 2\frac{\mu_{24}}{m_4}\vec{l}\cdot\vec{q}_1 + c_{24} - i\epsilon\right]}, \tag{B1}$$

$$I_1'[m_1, m_2, m_3, m_4] = \frac{-\mu_{12}\mu_{23}\mu_{24}}{2} \int \frac{d^3 l}{(2\pi)^3} \frac{1}{[\vec{l}^2 + c_{12} - i\epsilon] \left[\vec{l}^2 + 2\frac{\mu_{23}}{m_3}\vec{l}\cdot\vec{q}_3 + c_{23} - i\epsilon\right] \left[\vec{l}^2 - 2\frac{\mu_{24}}{m_4}\vec{l}\cdot\vec{q}_2 + c_{24}' - i\epsilon\right]}, \tag{B2}$$

$$\begin{aligned} I_2[m_1, m_2, m_3, m_4] = \frac{-\mu_{12}\mu_{34}}{2} \int \frac{d^3 l}{(2\pi)^3} &\frac{1}{[\vec{l}^2 + c_{12} - i\epsilon][\vec{l}^2 - \frac{2\mu_{34}}{m_4}\vec{l}\cdot\vec{q}_1 + \frac{2\mu_{34}}{m_3}\vec{l}\cdot\vec{q}_2 + c_{34} - i\epsilon]} \\ &\times \left[\frac{\mu_{24}}{[\vec{l}^2 - \frac{2\mu_{24}}{m_4}\vec{l}\cdot\vec{q}_1 + c_{24} - i\epsilon]} + \frac{\mu_{13}}{[\vec{l}^2 + \frac{2\mu_{13}}{m_3}\vec{l}\cdot\vec{q}_2 + c_{13} - i\epsilon]} \right]. \end{aligned} \tag{B3}$$

The parameters $c_{ij}^{(\prime)}$ in Eqs. (B1)–(B3) are defined as

$$c_{12} \equiv 2\mu_{12}(m_1 + m_2 - M), \tag{B4}$$

$$c_{23} \equiv 2\mu_{23}\left(m_2 + m_3 - M + q_1^0 + q_2^0 + \frac{\vec{q}_3^2}{2m_3}\right), \tag{B5}$$

$$c_{24} \equiv 2\mu_{24}\left(m_2 + m_4 - M + q_1^0 + \frac{\vec{q}_1^2}{2m_4}\right), \tag{B6}$$

$$c_{24}' \equiv 2\mu_{24}\left(m_2 + m_4 - M + q_2^0 + \frac{\vec{q}_2^2}{2m_4}\right) \tag{B7}$$

$$c_{34} \equiv 2\mu_{34}\left(m_3 + m_4 - q_3^0 + \frac{\vec{q}_1^2}{2m_4} + \frac{\vec{q}_2^2}{2m_3}\right), \tag{B8}$$

$$c_{13} \equiv 2\mu_{13}\left(m_1 + m_3 - M + q_2^0 + \frac{\vec{q}_2^2}{2m_3}\right). \tag{B9}$$

Note that the factor $m_1 m_2 m_3 m_4$ has canceled with the nonrelativistic normalization factors from the intermediate charmed mesons, which is different from the Refs. [60, 74].

Appendix C: Cutoff in scalar 4-point loop integrals

In this appendix, we discuss the parametrization and simplification of the scalar four-point integrals in the box diagrams. Taken the integral in Eq. (B1) as example, which is

$$\begin{aligned}&\int\frac{d^3l}{(2\pi)^3}\frac{1}{\left[\vec{l}^2+c_{12}-i\epsilon\right]\left[\vec{l}^2+2\frac{\mu_{23}}{m_3}\vec{l}\cdot\vec{q}_3+c_{23}-i\epsilon\right]\left[\vec{l}^2-2\frac{\mu_{24}}{m_4}\vec{l}\cdot\vec{q}_1+c_{24}-i\epsilon\right]}\\&=\frac{1}{(2\pi)^3}\int_0^{2\pi}\mathrm{d}\phi\int_{-1}^{1}\mathrm{d}x\int_0^{\Lambda}\mathrm{d}l\frac{l^2}{[l^2+c_{12}-i\epsilon][l^2+2\frac{\mu_{23}}{m3}\vec{l}\cdot\vec{q}_3+c_{23}-i\epsilon][-2\frac{\mu_{24}}{m_4}lq_1][x-x_0+i\epsilon]}\end{aligned}\tag{C1}$$

where $x_0=(l^2+c_{24})/(2\frac{\mu_{24}}{m_4}lq_1)$ and Λ is a cutoff.

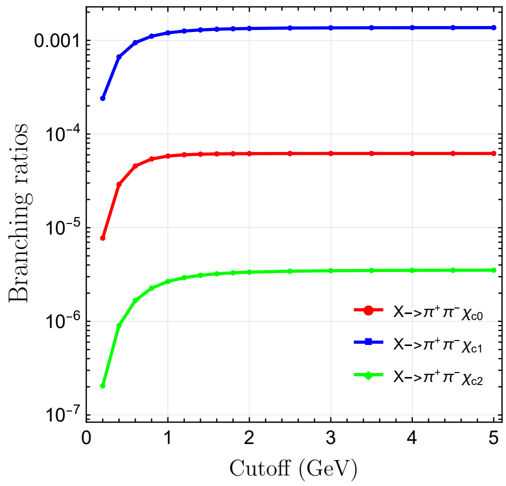

FIG. 4: The cutoff dependence of the branching ratios of $X(3872)\to\pi^+\pi^-\chi_{cJ}$ $(J=0,1,2)$ when we take $\theta=\pi/12$.

From Fig. 4, the branching ratios of $X(3872)\to\pi^+\pi^-\chi_{cJ}$ $(J=0,1,2)$ increase rapidly with the cutoff Λ below 1.5 GeV, reflecting significant low-momentum contributions. This scale coincides with the chiral symmetry breaking scale $\Lambda_\chi\approx 4\pi f_\pi=1.66$ GeV in HHχPT. For $\Lambda>1.5$ GeV, the growth slows and stabilizes, supporting the robustness of our approach. In Refs. [28, 31], the decays $X(3872)\to\chi_{cJ}(\pi^0,\pi\pi)$ were studied using HHχPT and X-EFT with the power divergence subtraction (PDS) scheme, reporting only the ratios $\frac{\mathrm{Br}[X(3872)\to\chi_{cJ}\pi\pi]}{\mathrm{Br}[X(3872)\to\chi_{cJ}\pi]}$ without specifying the cutoff Λ_{PDS}. Our work employs HHχPT with a hard momentum cutoff Λ, which generally differs from the PDS scheme by a factor. Using the upper limits of $\mathrm{Br}[X(3872)\to\chi_{c1/2}\pi^0]$ estimated from Ref. [71], we estimate the ratios $\frac{\mathrm{Br}[X(3872)\to\chi_{cJ}\pi^+\pi^-]}{\mathrm{Br}[X(3872)\to\chi_{cJ}\pi^0]}$ to be $2.28^{+11.2}_{-1.98}\times10^{-2}$ and $7.00^{+34.6}_{-6.00}\times10^{-5}$ for $J=1$ and 2, respectively. Our results are approximately a factor of 4 larger than those in Refs. [28, 31]. This corresponds to $\Lambda\approx 300$ MeV in our calculation. The factorization approach is limited by the charged channel binding momentum $\gamma_c\approx 126$ MeV. For $\Lambda\gg\gamma_c$, the wave function becomes unreliable in high-momentum regions, preventing recovery of factorization results. The estimated value $\Lambda\approx 300$ MeV is of the same order as γ_c and thus remains reasonable.

[1] S. K. Choi et al. (Belle), Phys. Rev. Lett. **91**, 262001 (2003), hep-ex/0309032.
[2] H.-X. Chen, W. Chen, X. Liu, and S.-L. Zhu, Phys. Rept. **639**, 1 (2016).
[3] A. Hosaka, T. Iijima, K. Miyabayashi, Y. Sakai, and S. Yasui, PTEP **2016**, 062C01 (2016).
[4] R. F. Lebed, R. E. Mitchell, and E. S. Swanson, Prog. Part. Nucl. Phys. **93**, 143 (2017).
[5] A. Esposito, A. Pilloni, and A. D. Polosa, Phys. Rept. **668**, 1 (2017).
[6] F.-K. Guo, C. Hanhart, U.-G. Meißner, Q. Wang, Q. Zhao, and B.-S. Zou, Rev. Mod. Phys. **90**, 015004 (2018), [Erratum: Rev.Mod.Phys. 94, 029901 (2022)].
[7] A. Ali, J. S. Lange, and S. Stone, Prog. Part. Nucl. Phys. **97**, 123 (2017).
[8] S. L. Olsen, T. Skwarnicki, and D. Zieminska, Rev. Mod. Phys. **90**, 015003 (2018).
[9] M. Karliner, J. L. Rosner, and T. Skwarnicki, Ann. Rev. Nucl. Part. Sci. **68**, 17 (2018).
[10] C.-Z. Yuan, Int. J. Mod. Phys. A **33**, 1830018 (2018).

[11] Y. Dong, A. Faessler, and V. E. Lyubovitskij, Prog. Part. Nucl. Phys. **94**, 282 (2017).
[12] Y.-R. Liu, H.-X. Chen, W. Chen, X. Liu, and S.-L. Zhu, Prog. Part. Nucl. Phys. **107**, 237 (2019).
[13] M.-Z. Liu, Y.-W. Pan, Z.-W. Liu, T.-W. Wu, J.-X. Lu, and L.-S. Geng (2024), 2404.06399.
[14] R. Aaij et al. (LHCb), Phys. Rev. D **92**, 011102 (2015), 1504.06339.
[15] S. Godfrey and N. Isgur, Phys. Rev. D **32**, 189 (1985).
[16] N. A. Tornqvist, Z. Phys. C **61**, 525 (1994), hep-ph/9310247.
[17] M. B. Voloshin, Phys. Lett. B **579**, 316 (2004), hep-ph/0309307.
[18] E. S. Swanson, Phys. Lett. B **588**, 189 (2004), hep-ph/0311229.
[19] N. A. Tornqvist, Phys. Lett. B **590**, 209 (2004), hep-ph/0402237.
[20] S. Fleming, M. Kusunoki, T. Mehen, and U. van Kolck, Phys. Rev. D **76**, 034006 (2007), hep-ph/0703168.
[21] Y.-R. Liu, X. Liu, W.-Z. Deng, and S.-L. Zhu, Eur. Phys. J. C **56**, 63 (2008), 0801.3540.
[22] E. S. Swanson, Phys. Lett. B **598**, 197 (2004), hep-ph/0406080.
[23] E. Braaten and M. Kusunoki, Phys. Rev. D **69**, 074005 (2004), hep-ph/0311147.
[24] E. Braaten and M. Kusunoki, Phys. Rev. D **71**, 074005 (2005), hep-ph/0412268.
[25] E. Braaten and M. Kusunoki, Phys. Rev. D **72**, 054022 (2005), hep-ph/0507163.
[26] X. Liu, B. Zhang, and S.-L. Zhu, Phys. Lett. B **645**, 185 (2007), hep-ph/0610278.
[27] S. Dubynskiy and M. B. Voloshin, Phys. Rev. D **77**, 014013 (2008), 0709.4474.
[28] S. Fleming and T. Mehen, Phys. Rev. D **78**, 094019 (2008), 0807.2674.
[29] Y.-b. Dong, A. Faessler, T. Gutsche, and V. E. Lyubovitskij, Phys. Rev. D **77**, 094013 (2008), 0802.3610.
[30] C. Bignamini, B. Grinstein, F. Piccinini, A. D. Polosa, and C. Sabelli, Phys. Rev. Lett. **103**, 162001 (2009), 0906.0882.
[31] S. Fleming and T. Mehen, Phys. Rev. D **85**, 014016 (2012), 1110.0265.
[32] F. Aceti, R. Molina, and E. Oset, Phys. Rev. D **86**, 113007 (2012), 1207.2832.
[33] A. Margaryan and R. P. Springer, Phys. Rev. D **88**, 014017 (2013), 1304.8101.
[34] F.-K. Guo, C. Hanhart, U.-G. Meißner, Q. Wang, and Q. Zhao, Phys. Lett. B **725**, 127 (2013), 1306.3096.
[35] F. K. Guo, C. Hidalgo-Duque, J. Nieves, A. Ozpineci, and M. P. Valderrama, Eur. Phys. J. C **74**, 2885 (2014), 1404.1776.
[36] Z.-Y. Zhou, M.-T. Yu, and Z. Xiao, Phys. Rev. D **100**, 094025 (2019), 1904.07509.
[37] Q. Wu, D.-Y. Chen, and T. Matsuki, Eur. Phys. J. C **81**, 193 (2021), 2102.08637.
[38] L. Meng, G.-J. Wang, B. Wang, and S.-L. Zhu, Phys. Rev. D **104**, 094003 (2021), 2109.01333.
[39] Y. Wang, Q. Wu, G. Li, W.-H. Qin, X.-H. Liu, C.-S. An, and J.-J. Xie, Phys. Rev. D **106**, 074015 (2022), 2209.12206.
[40] Q. Wu, M.-Z. Liu, and L.-S. Geng, Eur. Phys. J. C **84**, 147 (2024), 2304.05269.
[41] K. Abe et al. (Belle), in *22nd International Symposium on Lepton-Photon Interactions at High Energy (LP 2005)* (2005), hep-ex/0505037.
[42] M. Ablikim et al. (BESIII), Phys. Rev. Lett. **122**, 232002 (2019), 1903.04695.
[43] P. del Amo Sanchez et al. (BaBar), Phys. Rev. D **82**, 011101 (2010), 1005.5190.
[44] R. Aaij et al. (LHCb), Phys. Rev. D **108**, L011103 (2023), 2204.12597.
[45] Y. Yamaguchi, A. Hosaka, S. Takeuchi, and M. Takizawa, J. Phys. G **47**, 053001 (2020), 1908.08790.
[46] G.-J. Wang, Z. Yang, J.-J. Wu, M. Oka, and S.-L. Zhu, Sci. Bull. **69**, 3036 (2024), 2306.12406.
[47] J. Song, L. R. Dai, and E. Oset, Phys. Rev. D **108**, 114017 (2023), 2307.02382.
[48] D. Gamermann, J. Nieves, E. Oset, and E. Ruiz Arriola, Phys. Rev. D **81**, 014029 (2010), 0911.4407.
[49] D. Gamermann and E. Oset, Eur. Phys. J. A **33**, 119 (2007), 0704.2314.
[50] D. Gamermann and E. Oset, Eur. Phys. J. A **36**, 189 (2008), 0712.1758.
[51] D. Gamermann and E. Oset, Phys. Rev. D **80**, 014003 (2009), 0905.0402.
[52] D. Gamermann, C. E. Jimenez-Tejero, and A. Ramos, Phys. Rev. D **83**, 074018 (2011), 1011.5381.
[53] Y. Dong, A. Faessler, T. Gutsche, S. Kovalenko, and V. E. Lyubovitskij, Phys. Rev. D **79**, 094013 (2009), 0903.5416.
[54] M. Ablikim et al. (BESIII), Phys. Rev. Lett. **122**, 202001 (2019), 1901.03992.
[55] S. Navas et al. (Particle Data Group), Phys. Rev. D **110**, 030001 (2024).
[56] M. Ablikim et al. (BESIII), Phys. Rev. D **105**, 072009 (2022), 2202.00759.
[57] M. Ablikim et al. (BESIII), Phys. Rev. D **109**, L071101 (2024), 2312.13593.
[58] M. Ablikim et al. (BESIII), Phys. Rev. D **110**, 072015 (2024), 2408.01597.
[59] N. N. Achasov and G. N. Shestakov, Phys. Rev. D **110**, 016023 (2024), 2405.09228.
[60] Z.-S. Jia, Z.-H. Zhang, W.-H. Qin, and G. Li, Phys. Rev. D **109**, 034017 (2024), 2311.15527.
[61] S.-D. Liu, F. Wang, Z.-S. Jia, G. Li, X.-H. Liu, and J.-J. Xie, Phys. Rev. D **110**, 054048 (2024), 2406.01874.
[62] H.-D. Cai, Z.-S. Jia, G. Li, and S.-D. Liu, Phys. Rev. D **111**, 114024 (2025), 2503.20183.
[63] F.-K. Guo, C. Hanhart, and U.-G. Meissner, Phys. Rev. Lett. **103**, 082003 (2009), [Erratum: Phys.Rev.Lett. 104, 109901 (2010)], 0907.0521.
[64] F.-K. Guo, C. Hanhart, G. Li, U.-G. Meissner, and Q. Zhao, Phys. Rev. D **83**, 034013 (2011), 1008.3632.
[65] M. B. Wise, Phys. Rev. D **45**, R2188 (1992).
[66] J. Hu and T. Mehen, Phys. Rev. D **73**, 054003 (2006), hep-ph/0511321.
[67] T. Mehen, Phys. Rev. D **92**, 034019 (2015), 1503.02719.
[68] S. Weinberg, Phys. Rev. **137**, B672 (1965).
[69] V. Baru, J. Haidenbauer, C. Hanhart, Y. Kalashnikova, and A. E. Kudryavtsev, Phys. Lett. B **586**, 53 (2004), hep-ph/0308129.
[70] P. Colangelo, F. De Fazio, and T. N. Pham, Phys. Rev. D **69**, 054023 (2004), hep-ph/0310084.
[71] Z.-S. Jia, G. Li, and Z.-H. Zhang (2025), 2507.16618.
[72] F.-K. Guo, U.-G. Meißner, and Z. Yang, Phys. Lett. B **760**, 417 (2016), 1604.00770.
[73] M.-N. Tang, Y.-H. Lin, F.-K. Guo, C. Hanhart, and U.-G. Meißner, Commun. Theor. Phys. **75**, 055203 (2023), 2303.18225.
[74] Y.-H. Chen, Chin. Phys. C **44**, 023103 (2020), 1907.05547.